Soft Matter

RSC Publishing

PAPER

View Article Online
View Journal | View Issue

Cite this: *Soft Matter*, 2013, **9**, 9785

Photo-responsive cholesterol-substituted diacetylenic organogels: morphology tuning, photo-switching and photo-polymerization†

Jin Wang, Guang Yang, Hao Jiang, Gang Zou* and Qijin Zhang

Received 11th July 2013
Accepted 20th August 2013

DOI: 10.1039/c3sm51896e

www.rsc.org/softmatter

A novel cholesterol derivative organogelator (CAZODA) containing both azobenzene and diacetylenic units is synthesized. By using XRD, CD, TEM and SEM characterization, the gelation behavior, microscopic morphology and molecular packing structure in CAZODA assemblies are investigated in detail. It is found that the concentration of the CAZODA at the initial stage plays a crucial role in tuning the microstructure from helical fibers to spherulitic gel networks. Upon UV irradiation at 365 nm, the photo-induced transition of the helical packing structures for CAZODA assemblies has been demonstrated by CD characterization, and an explanation based on the co-assembly of both *trans*- and *cis*-form CAZODA has been proposed. In addition, upon irradiation at 254 nm for 3 h, the above organogel can be polymerized with concomitant color change from yellow to red. The polymerized gel exhibits enhanced stability upon thermo or photo-stimuli.

Introduction

Low-molecular-weight organogelators (LMOGs)[1,2] capable of immobilizing various organic solvents and even soft solids[3,4] have attracted increasing attention in the past decades because of their potential applications in photo-voltaics,[5] light-harvesting materials,[6] templates for preparation of the designed one-dimensional nanostructures,[7] drug controlled release,[8] fluorescent imaging and sensing[9] and so on. The driving forces for the spontaneous formation of the three-dimensional gel networks can be non-covalent interactions, including hydrogen bonding,[10] π–π stacking,[11] electrostatic,[12] dipole–dipole[13] and van der Waals interactions.[14] Among them, cholesterol-based gelators form a versatile category that has been systematically studied as cholesteryl groups can easily self-assemble through weak van der Waals interactions.[15–17] Besides, the interfacial tension caused by the presence of stereogenic centres usually leads to twisted assemblies.[18,19] Thus the above organogels always show optical activity as a result of the stacking of cholesterol units, and helical morphology can often be observed. The emergence of helical morphology built up from chiral molecular and macromolecular components is a familiar yet poorly understood phenomenon. In addition, stimuli-responsive gels are particularly important owing to their various potential applications.[20] Besides natural thermal stimuli, the gel–sol transition of organogels can be controlled reversibly or irreversibly by other stimuli such as light,[21] pH,[22] enzyme[23] and so on. Among the vast stimuli-responsive gels, azobenzene gelators play an important part benefiting from light triggered *trans–cis* isomerization.[24–26] Recently, we reported a photo-induced reversible dicholesterol-linked azobenzene organogel (DCAZO2) formed mainly by van der Waals interactions.[21,27] In this paper, another novel cholesterol-based gelator has been designed and synthesized. And we report new and remarkable findings concerning the preparation of the helical fibers, and how their helical packing structure can be altered by controlling the processing conditions or upon external photo-stimuli.

Recently, diacetylene-containing organogelators have attracted much interest as their noncovalently organized fibrous structures can be photo-polymerized through 1,4-addition reactions among the diyne groups, which leads to stable, covalently linked polydiacetylene networks.[28–33] To date, only a few papers describing diacetylene-based gelators have been reported, including cholesteryl ester,[34] glucosamide,[35] and lipid derivatives.[36] On the other hand, a programmed supramolecular approach to design and construct special one-dimensional nanostructures *via* a self-template approach has received much attention in the last couple of decades.[32] The amide group is widely used to properly orient butadiyne moieties in gel forms since the intermolecular distance between amide groups of molecules facing each other is *ca.* 4.8 Å, which is close to the butadiyne distance necessary to achieve a topochemical reaction. Upon photo-polymerization of the diacetylenic moieties, the designed gel networks can be stabilized and we expect the creation of a novel PDA supramolecular architecture *via* this self-template approach.

CAS Key Laboratory of Soft Matter Chemistry, Department of Polymer Science and Engineering, Key Laboratory of Optoelectronic Science and Technology in Anhui Province, University of Science and Technology of China, Hefei, Anhui 230026, P. R. China. E-mail: gangzou@ustc.edu.cn

† Electronic supplementary information (ESI) available: Some other ^{1}H-NMR, Raman, TEM, CD of gels. See DOI: 10.1039/c3sm51896e

In the course of this study, a novel cholesterol based gelator (CAZODA) containing both azobenzene and diacetylenic units was designed and synthesized through two amide linkages. The fabrication of helical fibers and subsequent growth of spherulitic gel networks of the CAZODA gelator in ethyl acetate were characterized in detail. Upon irradiation at 365 nm or 435 nm, the reversible gel-to-sol transition and the corresponding changes in the molecular helical packing in the gel network were investigated in detail by using UV, CD, XRD and TEM techniques. In addition, upon irradiation at 254 nm, the topo-polymerization of the diacetylenic moieties in the gel networks occurred, which further enhanced the stability of the designed gel networks.

Experimental section

Materials

10,12-Tricosadiynoic acid (DA) (Tokyo Chemical Industry Co., Ltd.) was purified by recrystallization before use. *P*-Diaminoazobenzene (Beijing InnoChem Science & Technology Co., Ltd.) and cholesteryl chloroformate (Alfa Aesar China Co., Ltd.) were used without further purification. Tetrahydrofuran (THF), *n*-hexane, triethylamine and *N*,*N*-dimethylformamide (DMF) were purified before use. THF was dried by distillation from sodium. Triethylamine was purified by refluxing over CaH_2 for 24 h followed by distillation. DMF and *n*-hexane were dried with anhydrous $MgSO_4$ and then distilled under reduced pressure. Other solvents and reagents were of analytical reagent grade and used without further purification.

Preparation of compound CAZODA: a cholesterol derivative containing azobenzene and diacetylenic moieties through two amide linkages (CAZODA) was synthesized in analogy to a previously described procedure.[37] The synthetic route for the CAZODA is shown in Fig. 1. DA (450 mg, 1.8 mmol) was dissolved in THF (30 ml) and oxalyl chloride (0.5 ml, excess) was added dropwise. The resulting mixture was stirred at room temperature for 30 min and one drop of fresh DMF was added as a catalyst. The above mixture was sequentially stirred at room temperature for 5 h. Then THF and excess oxalyl chloride were removed by rotary evaporation. The traces of oxalyl chloride trapped were removed by co-evaporation with 5 ml *n*-hexane three times. The obtained acid chloride was dissolved in THF (15 ml) and then was added dropwise to the solution of *p*-diaminoazobenzene (250 mg, 1.2 mmol), 0.5 ml triethylamine and 30 ml THF. The resulting mixture was stirred at room temperature overnight and protected by a dry tube of $CaCl_2$. The product (AZODA) was purified by column chromatography (ethyl acetate/petroleum ether (60–90 °C) = 1/3). Then cholesteryl chloroformate (142 mg, 0.32 mmol) was dissolved in THF (30 ml) and then was added dropwise to the solution of AZODA (180 mg, 0.32 mmol), 0.5 ml triethylamine and 30 ml THF. The resulting mixture was stirred at room temperature overnight and the final product (CAZODA) was purified by column chromatography (chloroform/methanol = 200/1) to afford a yellow powder. CAZODA: yield: 33%. ^{1}H NMR (400 MHz; $CDCl_3$) is shown in Fig. S1:† 7.89 (dd like, AA′XX′, 4H, ArH), 7.67 (dd like, AA′XX′, 2H, ArH), 7.52 (dd like, AA′XX′, 2H, ArH), 7.28 (s, 1H, CONH), 6.73 (s, 1H, CONH), 5.42 (s, 1H, vinylic), 4.64 (m, 1H, oxyalkyl), 2.39–0.69 (m, 84H, cholesteryl and diacetylenic protons). ESI-MS: calcd for $C_{65}H_{97}N_4O_3$ [M + H]+, 982.48; found, 981.70.

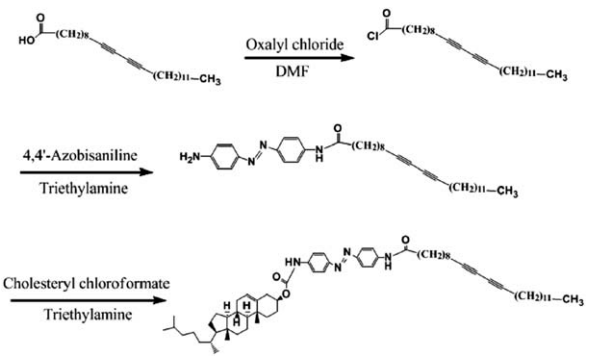

Fig. 1 Synthetic route for the cholesterol derivative containing azobenzene and diacetylenic moieties.

Characterization

The ^{1}H NMR spectrum was recorded on a Bruker 400 MHz NMR spectrometer (Bruker, Switzerland). UV-vis absorption spectra were measured by using a SHIMADZU UV-2550 PC spectrophotometer. Circular dichroism (CD) spectra were measured by using a JASCO J-810 spectropolarimeter. Optical cells (0.13 mm or 1 cm optical path length) were used for UV-vis and CD measurements. Photo-irradiation was carried out with a high-pressure mercury lamp (Hamamatsu LC6) through a UV or visible filter. The intensity of the UV light (365 nm) was about 1.9 mW cm^{-2}. X-ray diffraction (XRD) patterns were obtained on an MAC Science M18X X-ray diffractometer by using Cu K_α line ($\lambda = 0.154056$ nm). Scanning electron microscopy (SEM) was performed on a FEI Sirion200 system. The samples for SEM measurements were prepared by drop casting of the sample solution on silicon wafers and leaving them to dry in air. Transmission electron microscopy (TEM) images were obtained using a Hitachi H-7650 system at an accelerating voltage of 100 kV. The sample for TEM measurements was prepared by applying a drop of a sample solution on a copper grid and leaving it to dry in air. A 16 W UV lamp (λ = 254 nm, 0.5 mW cm^{-2}) hung 10 cm above the samples was used for photo-polymerization.

Gelation test

A weighted amount of the gelator and a measured volume of the selected pure organic solvent were placed into a sealed glass bottle and the solution was heated until the solid was dissolved. The solution was allowed to stand at room temperature for 1 h, and the state of the mixture was evaluated by the "stable to inversion of a test tube" method.[21]

Results and discussion

Gelation behavior

The gelation abilities were tested by heating and cooling the gel in different organic solvents. In general, it precipitated in nonpolar solvents but either gelated or dissolved well in polar

solvents. It was insoluble in *n*-hexane and cyclohexane. In tetrahydrofuran, cyclopentanone and dimethyl sulfoxide, the gel molecule was highly dissolved. Compared to similar cholesterol-linked azobenzene gelators,[21] we had deduced that the rigid diacetylene and amide moieties contribute to its poorer solubility in nonpolar solvents. Polar solvents were good for solubility but might break the noncovalent interactions. Thus a subtle compromise should be reached for gelation. Fortunately, turbid yellow gels formed successfully in the case of ethyl acetate and dioxane. The minimum gelation concentrations were 1% w/v and 2.5% w/v respectively. Ethyl acetate was chosen as the gelation solvent in other studies.

UV-vis absorption, CD spectra and XRD patterns

To obtain insights into the nature of the organized microstructures in the gel networks, normalized UV-vis absorption spectra and CD spectra characterization was performed. Compared with the normalized UV-vis absorption of the dilute solution, the π–π* transition band of the gel was broader, which could be caused by the H-type aggregates of azobenzene moieties (as shown in Fig. 2a). It indicated that there was strong aggregation between azobenzene groups in the organogel. We concluded that both H-type aggregates and isolated azobenzene moieties with widely varying angles θ existed in the organogel, which were responsible for the broadening of the spectrum in the near-UV range.[38] When the above organogel was subjected to CD characterization, it showed a negative exciton CD spectrum which consisted of the negative first Cotton effect (339 nm) and the positive second Cotton effect (313 nm), a sign of (*S*)-chirality (as shown in Fig. 2b). It is known that the cholesterol moiety with natural (*S*) C-3 configuration tends to give a negative first Cotton effect.[39,40] As for the dilute CAZODA solution, no obvious CD signals could be observed at the corresponding absorption band of the azobenzene moiety. All the above results indicated that the chiroptical properties of the organogel should be ascribed to the H-type aggregation of the azobenzene moiety, and the dipole moments of the azobenzene moiety tend to orient in the anticlockwise direction in the organogel.

Small- and wide-angle XRD studies were performed to determine the supramolecular structures of the ethyl acetate xerogel of CAZODA; the results are shown in Fig. 3. The formation of ordered structures in the CAZODA xerogel has been demonstrated by small angle XRD analysis. There are three scattering peaks corresponding to the distances of 6.72 nm, 3.26 nm and 1.67 nm (as shown in Fig. 3a). Considering that the second peak is more intense than the first one and the ratio of *d* values of the latter two peaks is very close to 2 : 1, we have indexed the three distances as (1,0), (0,1) and (0,2) of a 2D rectangular columnar structure. In the wide angle region (as shown in Fig. 3b), a π–π stacking peak at the value of 23.2° is observed, which corresponds to a spacing of 0.38 nm. All above results indicated that the diameter of the individual helical fiber should be about 7 nm.

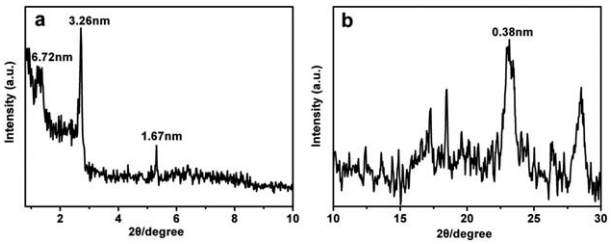

Fig. 3 (a) Small-angle and (b) wide-angle XRD patterns of the xerogel of CAZODA (1% w/v, in ethyl acetate).

Concentration-dependent construction of self-assembly morphology

In order to obtain a visual insight into the morphology of the molecular aggregation mode, a systematic study on the microstructure of different concentrations (from 0.2% to 1% w/v) of the CAZODA were conducted by TEM. It was worth noting that the concentration of CAZODA at the initial stage would play a crucial role in tuning the microstructure from helical nanofibers to three-dimensional spherulitic networks.

As shown in Fig. 4a and S2a,† when the concentration of the CAZODA solution was 0.2% w/v, left-handed helical nanofibers were observed growing in a one-dimensional way and some helical nanofibers crossed and fused into larger ones. The width of the thinnest nanofibers was about 14 nm, indicating that several fibers packed together to form larger bundles in this case.

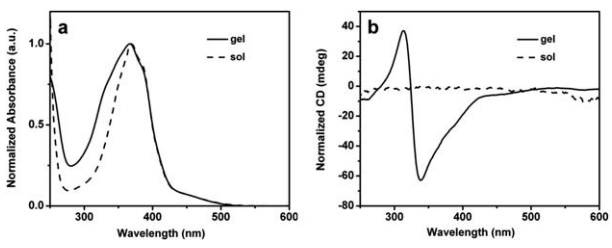

Fig. 2 (a) Normalized UV-vis spectra and (b) CD spectra of the CAZODA gel (1% w/v, in ethyl acetate, solid line) and the dilute solution (0.2% w/v, in ethyl acetate, dashed line).

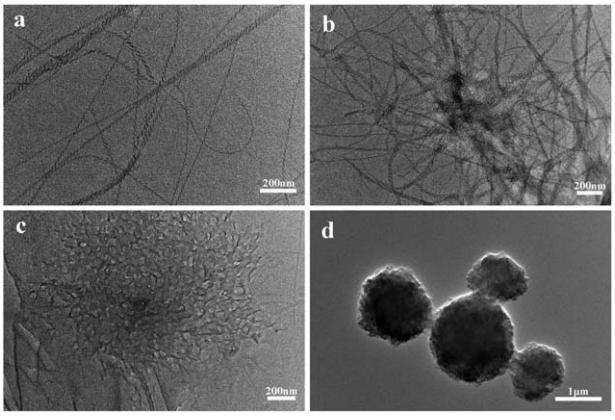

Fig. 4 TEM images of the topological self-assembly microstructure from the CAZODA solution: (a) 0.2% w/v, (b) 0.4% w/v, (c) 0.7% w/v and (d) 1% w/v in ethyl acetate.

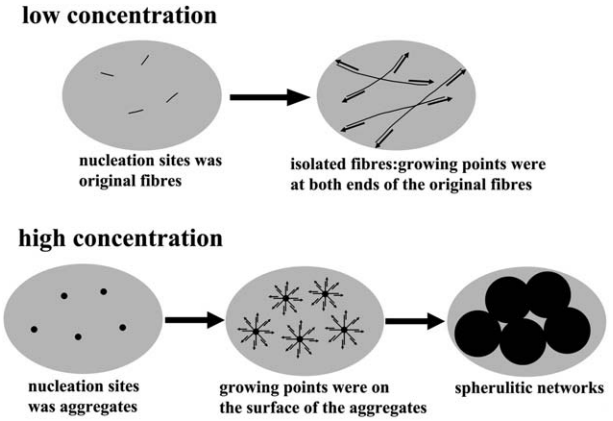

Fig. 5 Two different growth models for self-assembly of CAZODA.

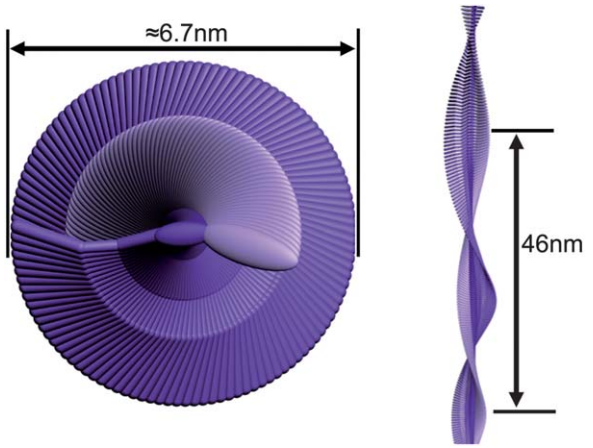

Fig. 6 Schematic representation of the CAZODA assemblies in (a) top and (b) side views.

The helical pitch of the fibers was about 46 nm. As shown in Fig. 4b, when the concentration was 0.4% w/v, more helical nanofibers with the same size were observed and crossed over with each other. Meanwhile, some nucleation sites appeared and nanofibers extended outward from the nucleation site radially. When the concentration was up to 0.7% w/v, the nanofibers around the nucleation site piled up, as shown in Fig. 4c. When the concentration was up to 1% w/v, some inter-connected globular particles about 2 μm in diameter were formed, which was in accordance with the results of SEM characterization (as shown in Fig. 4d and S2b†). The topological microstructure of the gel network didn't exhibit significant change when the concentration was higher than 1% w/v. SEM image and TEM image of a single globular particle showed the helical fibers at the edge of the globular particle (as shown in Fig. S3†). The concentration-dependent self-assembly morphology shown in Fig. 4 revealed two different growth models for self-assembly of CAZODA.[41] As schematically shown in Fig. 5, under low-concentration conditions, the nucleation sites were original fibers that consisted of a countable number of molecules and growing points were at both ends of the original fibers; so the growth of one-dimensional and isolated fibers was favored. Under high-concentration conditions, the nucleation sites were aggregates that consisted of many molecules and growing points were on the surface of the aggregates; so fibers grew extended outward from the nucleation site radially and piled up. Finally the inter-connected globular particles were formed and spherulitic networks were built up. It suggested that the concentration of CAZODA at the initial stage of gelation would play a crucial role in tuning the microstructure from helical nanofibers to three-dimensional spherulitic networks.

As mentioned above, the diameter of the individual nanofiber was about 7 nm, and the helical pitch was about 46 nm; so a helical period would contain 46/0.38 = 121 layers. This indicates that the first layer in a helical fiber would overlap geometrically with the 122nd layer. Considering that the length of a single molecule is about 5.7 nm (*trans* form of the CAZODA molecule), it is reasonable for one molecule in a single layer to construct the helical fiber through layer-by-layer stacking due to the coplanar configuration of CAZODA molecules. Based on the above TEM, XRD and CD data, a possible schematic model for supramolecular helical fibers is given in Fig. 6a (top view) and Fig. 6b (side view).

Photoisomerization of an azobenzene gelator

As we know, the azobenzene moiety is a well-known photosensitive chromophore, which undergoes photo-induced *trans* to *cis* isomerization upon irradiation at 365 nm, or *cis* to *trans* isomerization upon irradiation at 435 nm. Thus it was anticipated that the photo-isomerization of the azobenzene moieties might influence the molecular packing and optical properties of the CAZODA assemblies. After irradiation at 365 nm, the gel collapsed, together with the macroscopic gel to solution transition. Fig. 7a shows the variation of the UV-vis absorption spectra of the gel–sol transition upon irradiation at 365 nm. The π–π^* transition band in the near UV range of trans isomers with λ_{max} at 368 nm decreased gradually during irradiation at 365 nm, together with the macroscopic gel to sol transition. The gel collapsed and the breaking of van der Waals interactions occurred due to the large change in molecular geometry caused by the photoisomerization of the azobenzene moieties. After irradiation for 180 s, the UV-vis spectra didn't change anymore, indicating that the azobenzene moieties reached a *cis* saturated state (*ca.* 85%). The *cis* saturated CAZODA couldn't form a gel after keeping in dark overnight. In contrast, upon irradiation at 435 nm, the system was still dissolved partly and the UV-vis spectra of a *cis* CAZODA saturated solution were recovered by the reverse *cis*-to-*trans* isomerization after 380 s. The gel was reformed after heating and cooling treatment (as shown in Fig. S4†). Unlike the case in the dilute CAZODA solution, there was no isosbestic point between the two absorption bands, suggesting that there were H-type aggregates besides trans and isolated cis isomers of the azobenzene moieties existing in the reversible gel-to-sol and sol-to-gel transition.

The rate and degree of isomerization could be evaluated from the absorption spectra. Photo-isomerization of the azobenzene groups was a first-order reaction which could be analyzed by the following kinetic equation:

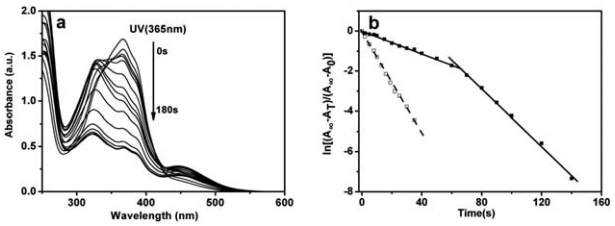

Fig. 7 (a) Variation of the UV-vis spectra of the gel of CAZODA (1% w/v, in ethyl acetate) upon irradiation at 365 nm and (b) the dependence of $\ln[(A_\infty - A_t)/(A_\infty - A_0)]$ on irradiation time for the gel of CAZODA (1% w/v, in ethyl acetate solid line) and its dilute solution (0.2% w/v, in ethyl acetate, dashed line).

$$\ln[(A_\infty - A_t)/(A_\infty - A_0)] = -kt \quad (1)$$

and the degree of isomerization R could be estimated from the following equation:

$$R = (A_0 - A_\infty)/A_0 \times 100\% \quad (2)$$

where A_0, A_t and A_∞ are the absorbances at the initial time, time t and the photo-stationary state, respectively. K is the photo-isomerization rate constant and t is the irradiation time. As shown in Fig. 7b, the plots of the dilute CAZODA solution could be well-fitted as a linear relationship and the corresponding first-order rate constant k_s was determined to be $0.128 \pm 0.002\ s^{-1}$. However, the plots of the gel could be divided into two stages. In the first stage, the first-order rate constant k_{g1} ($0.028 \pm 0.001\ s^{-1}$) was much smaller than that in solution, suggesting that there were much stronger intermolecular interactions in the gel state. In the second stage, the first-order rate constant k_{g2} ($0.072 \pm 0.002\ s^{-1}$) was much higher than k_{g1} but smaller than k_s. Therefore, the *trans–cis* photoisomerization of azobenzene moieties in the gel could be comprehended as follows: in the first stage, the isomerization process of partial moieties (in the H-type aggregate state) was hindered due to strong intermolecular interactions; when the isomerization process reached a specific degree (68%, calculated from the intersection point of the two fitted lines), the gel network was totally broken and the intermolecular interactions were much weakened, so the following isomerization process was significantly faster compared to the first stage. The relatively low conversion ratio from trans to cis isomer (*ca.* 85%) and strong H-type aggregation suggested that there wasn't sufficient free volume in the gel state for the photoisomerization of the azobenzene moieties to take place.

As shown in Fig. 8, the variation of the CD spectrum for the CAZODA assemblies upon irradiation at 365 nm could be divided into three stages. In the first stage, the original bisignate CD signal (339/313 nm, −/+) decreased with the increment of the irradiation time, and disappeared completely after 15 s (the degree of isomerization was estimated to be 27%). These results indicated that the ordered helical packing of the *trans*-form CAZODA in the gel state had been destroyed due to the large change of molecular geometry caused by the photoisomerization of the azobenzene moieties. When the irradiation time was in excess of 20 s, a novel bisignate CD signal (439/345 nm, −/+) appeared and increased with the increment of the irradiation

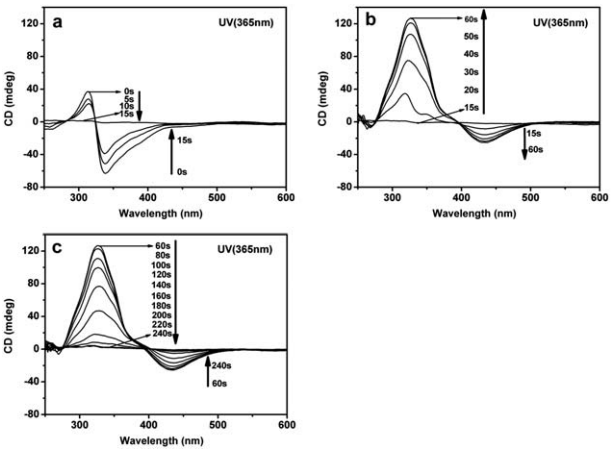

Fig. 8 Variation of the CD spectra of the gel of CAZODA (1% w/v, in ethyl acetate) upon irradiation at 365 nm.

time (<60 s). Interestingly, the emerging CD signal was much stronger than the original CD signal; however, it had shifted to higher wavelength. It is well-known that the emergence of a couplet Cotton effect is usually associated with coupling between the chromophores owing to π–π stacking. The above results indicated that the novel helical aggregates were only observed after a period of irradiation at 365 nm, suggesting that a relatively high concentration of the *cis*-form CAZODA was required for the emerging helical aggregates. When the isomerization process reached a specific degree, the cooperative stereoregular arrangement of both *trans*- and *cis*-form CAZODA occurred. The cooperative assembly of both *trans*- and *cis*-form CAZODA was assumed to contribute to the special overcrowded molecular packing into a helical sense, resulting in the formation of the emerging chirality (as shown in Fig. 9). Upon excess UV irradiation (the degree of isomerization, $R > 68\%$), most of the *trans*-form CAZODA transferred to the *cis* form, resulting in the disassembly of overcrowded molecular packing and the disappearance of the emerging CD signals. All above results indicated that a suitable concentration of the *cis*-form CAZODA and the overcrowded molecular packing into a helical sense seemed to play dominant roles in the formation of the chirality. This result was similar to that reported on the chirality obtained from the cooperative assembly of both *trans*- and *cis*-form azobenzene

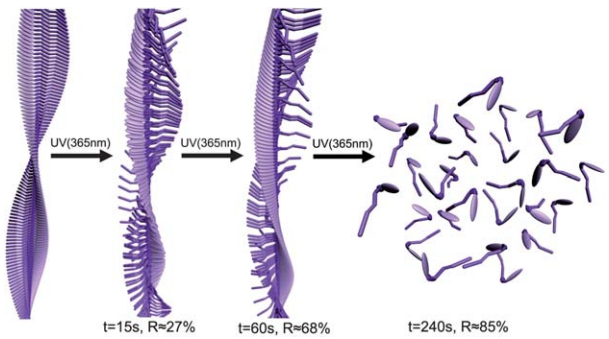

Fig. 9 The schematic representation of the photo-induced transition of the helical packing structures for CAZODA assemblies (1% w/v, in ethyl acetate).

derivatives.[42] Interestingly, upon irradiation at 435 nm for 20 min and after heating and cooling, the organogel could be reformed. The original bisignate CD signal (339/313 nm, −/+) also could recover (as shown in Fig. S5†), indicating the reformation of the initial helical packing of the *trans*-form CAZODA in the organogel.

Photo-polymerization

We performed the photo-polymerization of the ethyl acetate gel of CAZODA upon irradiation at 254 nm. The color of the gel changed from yellow to red upon irradiation at 254 nm. The appearance of the red color implied that polydiacetylene had been produced (as shown in Fig. S6†). No obvious shape change could be observed for the CAZODA gel sample before and after irradiation at 254 nm. After photo-irradiation at 254 nm for 280 min, the gel turned red and exhibited characteristic Raman vibrational bands at 2101 and 1501 cm^{-1}, corresponding to the C≡C and C=C stretching vibrations of the PDA backbone, respectively (as shown in Fig. S7†). All the above results confirmed the successful formation of the PDA structure in the organogel. Photo-polymerization of the gel could also be detected optically. Fig. 10a showed the variation of absorption spectra of the CAZODA gel during the photo-irradiation. The absorption band with a typical intense absorption maximum at 610 and 550 nm was observed after photo-polymerization on account of the conjugated PDA chain exhibiting typical intense absorption at about 600 and 550 nm. In the first stage, the absorption maximum proceeded rapidly up to about 0.63 and then reached 0.76 after 200 min. The longer irradiation time couldn't lead to a further increase in the absorption maximum. The absorption maximum against the exposure time is shown in Fig. 10b. The curves clearly indicated that the polymerization kinetics process of the gel could be described as a first order reaction, and the rate constant k for the gel was 0.0011 ± 0.0001 s^{-1}. No obvious self-acceleration phenomena could be observed for the photo-polymerization of the gel. All the above results confirmed the successful formation of the PDA structure in the organogel. Upon irradiation at 254 nm, the intensity of the CD signal for azobenzene moieties decreased gradually (as shown in Fig. S8†). The decrease of CD intensity resulted from the *trans–cis* photo-isomerization of azobenzene groups. However, no Cotton effect appeared at the corresponding absorption band of PDA main chains, which indicated that chirality transfer did not occur from the helical packing of the azobenzene moieties to the obtained PDA main chains.

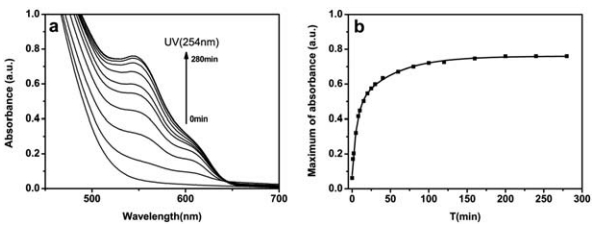

Fig. 10 (a) Variation of the UV-vis spectra of the gel of CAZODA (1% w/v, in ethyl acetate) upon irradiation at 254 nm and (b) the time resolved development of the absorption maximum at approximately 550 nm. The solid curve is the simulated curve described as a first order rate equation.

Photopolymerization increased the stability of the gel state. The stability of the polymerized gel was examined upon heating or UV irradiation at 365 nm. Before polymerization, the CAZODA gel transformed to a sol upon heating above 45 °C or UV irradiation at 365 nm for 5 min; however, the polymerized gel maintained the shape upon heating above 80 °C or longer irradiation time at 365 nm. The UV-vis spectral changes of the polymerized gel upon irradiation at 365 nm are shown in Fig. S9.† Upon irradiation at 365 nm for 120 s in this case, only a slight isomerization ratio (*ca.* 3.2%) was observed. In addition, no obvious change was observed at the corresponding absorption band of the PDA main chains. The polymerization of the diacetylenic moiety was assumed to keep the networks fixed by covalent bonding, which ensured "locking" of the side chain configurations, inhibiting the photo-isomerization of the azobenzene chromophore in this case. All the above results indicated that the polymerization of the gel could dramatically enhance its stability upon thermo or photo-stimuli.

Conclusions

In summary, we have synthesized a novel cholesterol based organic gelator that contains both azobenzene and diacetylenic moieties. The concentration of the CAZODA at the initial stage plays a crucial role in tuning the microstructure from the helical fibers to the spherulitic networks. Upon irradiation at 365 nm for 15 s, the initial helical packing of the *trans*-form CAZODA can be destroyed due to the photo-isomerization of the azobenzene units. When the isomerization process reaches a specific degree, the cooperative co-assembly of *trans*- and *cis*-form CAZODA isomers occurs, resulting in the formation of special overcrowded molecular packing with a novel helical form. The gel can be polymerized upon irradiation at 254 nm and the color changed from yellow to red. Our results reported herein not only provide new physical insights into the fabrication of the functional helical architectures, but are also of great fundamental value for the rational design of novel PDA assemblies *via* a self-template approach.

Acknowledgements

This research was carried out with funding from the National Natural Science Foundation of China (No: 51173176, 51273186, 21074123, 91027024), the Chinese Academy of Sciences (kjcx2-yw-m11) and the Fundamental Research Funds for the Central Universities (WK2060200008).

Notes and references

1 D. K. Smith, *Nat. Chem.*, 2010, **2**, 162–163.
2 D. K. Maiti and A. Banerjee, *Chem.–Asian J.*, 2013, **8**, 113–120.
3 M. Fahrländer, K. Fuchs, R. Mü1haupt and C. Friedrich, *Macromolecules*, 2003, **36**, 3749–3757.
4 B. Isare, L. Petit, E. Bugnet, R. Vincent, L. Lapalu, P. Sautet and L. Bouteiller, *Langmuir*, 2009, **25**, 8400–8403.
5 M. Carrasco-Orozco, W. C. Tsoi, M. O'Neill, M. P. Aldred, P. Vlachos and S. M. Kelly, *Adv. Mater.*, 2006, **18**, 1754–1758.

6 K. Sugiyasu, N. Fujita and S. Shinkai, *Angew. Chem., Int. Ed.*, 2004, **43**, 1229–1233.
7 M. Shirakawa, N. Fujita and S. Shinkai, *J. Am. Chem. Soc.*, 2005, **127**, 4164–4165.
8 G. L. Liang, Z. M. Yang, R. J. Zhang, L. H. Li, Y. J. Fan, Y. Kuang, Y. Gao, T. Wang, W. W. Lu and B. Xu, *Langmuir*, 2009, **25**, 8419–8422.
9 K. K. Kartha, S. S. Babu, S. Srinivasan and A. Ajayaghosh, *J. Am. Chem. Soc.*, 2012, **134**, 4834–4841.
10 S. Yagai, T. Nakajima, K. Kishikawa, S. Kohmoto, T. Karatsu and A. Kitamura, *J. Am. Chem. Soc.*, 2005, **127**, 11134–11139.
11 H. Shao and J. R. Parquette, *Chem. Commun.*, 2010, **46**, 4285–4287.
12 S. Taguchi, T. Matsumoto, T. Ichikawa, T. Katob and H. Ohno, *Chem. Commun.*, 2011, **47**, 11342–11344.
13 J. Mamiya, K. Kanie, T. Hiyama, T. Ikeda and T. Kato, *Chem. Commun.*, 2002, 1870–1871.
14 R. C. Kramb and C. F. Zukoski, *Langmuir*, 2008, **24**, 7565–7572.
15 Y. Lin and R. G. Weiss, *Macromolecules*, 1987, **20**, 414–417.
16 J. X. Peng, K. Q. Liu, J. Liu, Q. H. Zhang, X. L. Feng and Y. Fang, *Langmuir*, 2008, **24**, 2992–3000.
17 P. Chen, R. Lu, P. C. Xue, T. H. Xu, G. J. Chen and Y. Y. Zhao, *Langmuir*, 2009, **25**, 8395–8399.
18 S. Azeroual, J. Surprenant, T. D. Lazzara, M. Kocun, Y. Tao, L. A. Cuccia and J. M. Lehn, *Chem. Commun.*, 2012, **48**, 2292–2294.
19 A. Brizard, C. Aimé, T. Labrot, I. Huc, D. Berthier, F. Artzner, B. Desbat and R. Oda, *J. Am. Chem. Soc.*, 2007, **129**, 3754–3762.
20 A. Kavanagh, R. Byrne, D. Diamond and K. J. Fraser, *Membranes*, 2012, **2**, 16–39.
21 Y. P. Wu, S. Wu, X. J. Tian, X. Wang, W. X. Wu, G. Zou and Q. J. Zhang, *Soft Matter*, 2011, **7**, 716–721.
22 D. M. Wood, B. W. Greenland, A. L. Acton, F. R. Llansola, C. A. Murray, C. J. Cardin, J. F. Miravet, B. Escuder, I. W. Hamley and W. Hayes, *Chem.–Eur. J.*, 2012, **18**, 2692–2699.
23 Y. Z. Xing, E. J. Cheng, Y. Yang, P. Chen, T. Zhang, Y. W. Sun, Z. Q. Yang and D. S. Liu, *Adv. Mater.*, 2011, **23**, 1117–1121.
24 Y. Matsuzawa and N. Tamaoki, *J. Phys. Chem. B*, 2010, **114**, 1586–1590.
25 K. Murata, M. Aoki, T. Suzuki, T. Harada, H. Kawabata, T. Komri, F. Ohseto, K. Ueda and S. Shinkai, *J. Am. Chem. Soc.*, 1994, **116**, 6664–6676.
26 M. de Loos, J. van Esch, R. M. Kellogg and B. L. Feringa, *Angew. Chem., Int. Ed.*, 2001, **40**, 613–616.
27 Y. P. Wu, S. Wu, G. Zou and Q. J. Zhang, *Soft Matter*, 2011, **7**, 9177–9183.
28 K. Aoki, M. Kudo and N. Tamaoki, *Org. Lett.*, 2004, **6**, 4009–4012.
29 N. Fujita, Y. Sakamoto, M. Shirakawa, M. Ojima, A. Fujii, M. Ozaki and S. Shinkai, *J. Am. Chem. Soc.*, 2007, **129**, 4134–4135.
30 O. J. Duatel, M. Robitzer, J. Lère-Porte, F. Serein-Spirau and J. J. E. Moreau, *J. Am. Chem. Soc.*, 2006, **128**, 16213–16223.
31 J. R. Néabo, K. I. S. Tohoundjona and J. Morin, *Org. Lett.*, 2011, **13**, 1358–1361.
32 M. Shirakawa, N. Fujita and S. Shinkai, *J. Am. Chem. Soc.*, 2005, **127**, 4164–4165.
33 E. Jahnke, N. Severin, P. Kreutzkamp, J. P. Rabe and H. Frauenrath, *Adv. Mater.*, 2008, **20**, 409–414.
34 J. Nagasawa, M. Kudo, S. Hayashi and N. Tamaoki, *Langmuir*, 2004, **20**, 7907–7916.
35 M. Masuda, T. Hanada, Y. Okada, K. Yase and T. Shimizu, *Macromolecules*, 2000, **33**, 9233–9238.
36 M. George and R. G. Weiss, *Chem. Mater.*, 2003, **15**, 2879–2888.
37 Y. L. Wang, X. Chen, G. Zou and Q. J. Zhang, *Macromol. Chem. Phys.*, 2010, **211**, 888–896.
38 S. Wu, L. F. Niu, J. Shen, Q. J. Zhang and C. Bubeck, *Macromolecules*, 2009, **42**, 362–367.
39 M. Zinic, F. Vogtle and F. Fages, *Top. Curr. Chem.*, 2005, **256**, 39–76.
40 J. H. Jung, S. Shinkai and T. Shimizu, *Chem. Mater.*, 2003, **15**, 2141–2145.
41 R. Y. Wang, X. Y. Liu, J. Y. Xiong and J. L. Li, *J. Phys. Chem. B*, 2006, **110**, 7275–7280.
42 A. Gopal, M. Hifsudheen, S. Furumi, M. Takeuchi and A. Ajayaghosh, *Angew. Chem., Int. Ed.*, 2012, **51**, 10505–10509.